



**HAL**  
open science

## Authenticating teas using multielement signatures, strontium isotope ratios, and volatile compound profiling

Marine Reyrolle, Gilles Bareille, Ekaterina Epova, Julien Barre, Sylvain Bérail, Thierry Pigot, Valérie Desauziers, Lydia Gautier, Mickael Le Béhec

### ► To cite this version:

Marine Reyrolle, Gilles Bareille, Ekaterina Epova, Julien Barre, Sylvain Bérail, et al.. Authenticating teas using multielement signatures, strontium isotope ratios, and volatile compound profiling. *Food Chemistry*, 2023, 423, pp.136271. 10.1016/j.foodchem.2023.136271 . hal-04102107

**HAL Id: hal-04102107**

**<https://univ-pau.hal.science/hal-04102107>**

Submitted on 23 May 2023

**HAL** is a multi-disciplinary open access archive for the deposit and dissemination of scientific research documents, whether they are published or not. The documents may come from teaching and research institutions in France or abroad, or from public or private research centers.

L'archive ouverte pluridisciplinaire **HAL**, est destinée au dépôt et à la diffusion de documents scientifiques de niveau recherche, publiés ou non, émanant des établissements d'enseignement et de recherche français ou étrangers, des laboratoires publics ou privés.

# Authenticating teas using multielement signatures, strontium isotope ratios, and volatile compound profiling.

Marine Reyrolle<sup>a</sup>, Gilles Bareille<sup>a</sup>, Ekaterina N. Epova<sup>b</sup>, Julien Barre<sup>b</sup>, Sylvain Bérail<sup>b</sup>,  
Thierry Pigot<sup>a</sup>, Valerie Desauziers<sup>a</sup>, Lydia Gautier<sup>c</sup> and Mickael Le Behec<sup>a\*</sup>

<sup>a</sup> Université de Pau et des Pays de l'Adour, E2S UPPA, CNRS, IMT Mines Ales, IPREM, Pau, France, Institut des sciences analytiques et de Physicochimie pour l'environnement et les Matériaux, UMR5254, Hélioparc, 2 avenue du Président Angot, 64053, Pau cedex 9, France

<sup>b</sup> Advanced Isotopic Analysis (A.I.A.), Hélioparc, 2 avenue du Président Angot, 64000, Pau, France

<sup>c</sup> T Edition, 63 rue Vercingétorix, 75014 Paris, France

*\*Corresponding author at Université de Pau et des Pays de l'Adour, E2S UPPA, CNRS, IMT Mines Ales, IPREM, Pau, France*

*Email adress : [mickael.lebehec@univ-pau.fr](mailto:mickael.lebehec@univ-pau.fr) Phone: +335 59 40 75 84*

---

## Abstract

High value food products are subject to adulterations and frauds. This study aimed to combine, in our knowledge for the first time, inorganic chemical tracers (multi-elements and Sr isotopy) with volatile organic compound (VOCs) to discriminate the geographic origin, the varieties and transformation processes to authenticate 26 tea samples. By measuring Sr isotope ratio using the multi-collector inductively coupled plasma mass spectrometry (MC-ICP-MS), 6 out of 11 regions were successfully discriminated. The combination with the ICP-MS inorganic pattern allowed to discriminate 4 more regions with a significance level of 0.05. VOCs fingerprints, obtained with selected ion flow tube mass spectrometer (SIFT-MS), were not correlated with origin but with the cultivar and transformation processes. Green, oolong, and dark teas were clearly differentiated, with hexanal and hexanol contributing to the discrimination of oxidation levels. With this multi-instrumental approach, it is possible to certify the geographical origin and the tea conformity.

---

## Highlights

- VOCs profiles, <sup>87</sup>Sr/<sup>86</sup>Sr ratio and multielement analysis were applied on tea
- <sup>87</sup>Sr/<sup>86</sup>Sr ratio discriminated 6 of the 11 regions of the sample collection
- Inorganic pattern improved the discrimination of Sr isotope ratio up to 10
- Volatile fingerprints were mainly impacted by the type of Camelia cultivar
- Hexanal and hexanol were highlighted for the classification with oxidation rate

## 33 Keywords

34 Tea, traceability, authenticity of food products, inorganic pattern, volatile organic compounds  
35 profiling, Sr isotope ratio

---

36

37

## 38 1. Introduction

39 Food provenance assessment is a global concern for sanitary and quality control. Consumers expect  
40 more guarantees regarding food quality, i.e., information on composition, absence of health risks,  
41 product origin, quality, and transformation processes with reduced environmental impact. Thus, labels  
42 have been developed to meet these expectations providing information regarding the product origin  
43 (Protected Designation of Origin (PDO) and Protected Geographical Indication (PGI)) along with  
44 environmental and social impact. These labels, provided by authorities, authenticate agri-food  
45 products regarding product origin and expected sensory quality. Unfortunately, certified products are  
46 *de facto* more expensive and profitable, which encourages the fraud development and fake products  
47 in the marketplace. This problem is particularly acute for old products consumed worldwide, such as  
48 tea.

49 For centuries, people have consumed tea and enjoyed its taste and aroma. Originally produced in  
50 China, tea is now mainly produced in Asia (India, China, Sri Lanka, Vietnam, and Japan), but also in  
51 Africa (Kenya) and in South America. Tea plants, *Camellia sinensis* (*C. sinensis*), are members of the  
52 family *Theaceae*. The first wild tea plants grew at the source of the Irrawaddy River in a triangle formed  
53 by Yunnan in China, Northeast India, Burma, and Tibet. Tea plants have spread naturally along rivers,  
54 giving rise to three main varieties: *sinensis*, *assamica*, and *cambodiensis*. Various national research  
55 institutes developed new varieties that were more adapted to local climatic conditions (e.g., resistant  
56 to certain pests, early or mature growth) and balanced productivity and quality. Thus, a large number  
57 of cultivars were created via cutting, grafting, layering, or suckering. The terroir, i.e., the composition  
58 of soil, climate, altitude, latitude, the plants grown alongside tea plants, picking methods and periods  
59 all play an essential role in developing the organoleptic qualities of tea.

60 Moreover, many changes in the transformation processes of *C. sinensis* leaves have led to the  
61 development of several types of tea (Feng et al., 2019). Therefore, based on the drying, fixation,  
62 fermentation, and enzymatic oxidation levels, teas can be classified into different colours: green, black,  
63 dark, red, white, oolong and yellow (Zhang et al., 2019). Nevertheless, only a few labels have been  
64 created, such as Darjeeling tea, a typical black tea from North India, which is one of the most famous  
65 teas. Currently, only 10,000 tons of Darjeeling tea is produced annually, while four times as much is  
66 sold worldwide. This information highlights the challenge of traceability of high-value food products.  
67 Beyond the product-origin information, consumers also want to be informed about typical product  
68 quality.

69 To protect producers, manufacturers, and consumers, labelled products must be cultivated and  
70 transformed in a defined geographic area. In order to obtain a label in addition to the declarative  
71 aspect, several fraud checks should be conducted by food industry sectors to assess product origin.  
72 The development of new analytical techniques for determining the geographical origin and  
73 authenticity of products has increased since the 1980s. Such techniques include stable isotopes,  
74 analysis of carbon, nitrogen, and oxygen, near-infrared spectroscopy, nuclear magnetic resonance  
75 spectroscopy, electronic nose sensing, multielement analysis, chromatographic techniques, evaluation

76 by mass spectrometry and sensory analysis (Luykx & van Ruth, 2008). Recent reviews gave a state of  
77 art of methods to trace the origin and quality of foods produced in China, including tea (Li et al., 2023;  
78 Shuai et al., 2022).

79 Inductively coupled plasma mass spectrometry (ICP-MS) is widely used in multielement fingerprinting  
80 for the geographical assessment of various plant-based food products, such as olive oil (Nasr et al.,  
81 2021), coffee (Liu et al., 2014), wine (Epova et al., 2020), and tea (Liu et al., 2021). Plants grow in soil  
82 containing organic and mineral matter as well as water. Mineral elements are transferred to the plant  
83 tissues during cultivation and lead to different multielement signatures depending on product origin  
84 that reflect underlying geology and soil composition (Liu et al., 2021). Anthropogenic actions and  
85 environmental pollution may also contribute to elemental signatures (Zhao et al., 2017). Inorganic  
86 elements, such as Sr, Pb, B, Cd, Li, Na, Mg, Al, K, Ca, V, Cr, Mn, Fe, Co, Ni, Cu, Zn, As, Rb, and Ba, may  
87 be good tea leaves markers before and after processing (Gomes et al., 2019). Moreover, post-  
88 processing (drying or roasting) and storage methods are more likely to affect the active organic  
89 compounds that may degrade or attenuate (Ni et al., 2018). Sr and especially the ratio of two of its  
90 four isotopes ( $^{87}\text{Sr}/^{86}\text{Sr}$ ) has an advantage over element contents. Indeed, it has been shown that the  
91  $^{87}\text{Sr}/^{86}\text{Sr}$  isotope ratio does not change during biological processes (no biological fractionation) and, in  
92 plants, reflects the growth environment: mainly the bioavailable fraction of Sr derived from the  
93 mineral weathering processes of bedrock and soil (Bin et al., 2022), although atmospheric and  
94 anthropogenic sources, e.g., fertilisers, may sometimes play a role (Bataille et al., 2020).

95 In addition to geographic origin, consumers expect the taste and aroma of teas to match the label. This  
96 quality aspect of tea is closely related to agricultural practices, including growth and harvest  
97 conditions, as well as transformation processes and storage conditions. Tea experts can assess the  
98 expected quality of labelled samples, but this ability requires a long learning process. Analytical  
99 chemistry methods were thus developed to monitor the characteristic markers of types of tea (Lin et  
100 al., 2013; Zhang et al., 2013). Recently, a new global approach based on the identification of volatile  
101 compound fingerprints for product traceability has been developed using proton-transfer reaction-  
102 mass spectrometry (PTR-MS) (Yener et al., 2016). This method features the nontargeted measurement  
103 of volatile organic compounds (VOCs) emitted by a product using a rapid and non-destructive mass  
104 spectrometer with a soft chemical ionization source. Selected ion flow tube mass spectrometry (SIFT-  
105 MS) is also a direct-injection mass spectrometry (DIMS) technique that determine the volatile  
106 fingerprint of a product by monitoring the ions produced by volatile molecules and eight chemical  
107 precursors (Reyrolle et al., 2022).

108 Throughout this study, we performed and combined for the first time on a collection of tea samples,  
109 multielement signature measurements using ICP-MS, Sr isotope ratio with multi collector ICP-MS and  
110 SIFT-MS volatile fingerprints to trace origin of production, cultivar type, transformation processes and  
111 therefore conformity. For this purpose, it was essential to work with tea samples with perfectly  
112 certified origins. To conduct this study, our collaborator, a tea expert collected 26 samples directly  
113 from the producers and factories in order to avoid blending along supply chain.

114

## 115 2. Material and methods

116

### 117 2.1. Samples

118 A tea expert collected 26 tea samples (Table 1) with certified origins directly from producers or  
 119 factories, from 2011 to 2020. These tea samples were obtained from six countries: Nepal (n = 3), China  
 120 (n = 11), Vietnam (n = 5), India (n = 3), Sri Lanka (n = 2), and Japan (n = 2), corresponding to 11 regions  
 121 (Figure SI1). These tea samples displayed five colours: green (n = 6), black (n = 10), dark (n = 3), white  
 122 (n = 4), and oolong (n = 3). Samples were stored in sealed aluminium bags (Jamo solution LTD,  
 123 Orpington, Kent, United Kingdom) at 25°C ± 5 in the dark.

124

125

Sample	Country	Region	Colour	Cultivars
Tea-1	Nepal	Ilam Valley	White	Mix Clonal Cultivars
Tea-2	Nepal	Ilam Valley	White	Mix Clonal Cultivars
Tea-3	Nepal	Ilam Valley	White	Mix Clonal Cultivars
Tea-4	China	Zhejiang	Green	Jiu Hang
Tea-5	China	Zhejiang	Green	Jiu Hang
Tea-6	China	Zhejiang	Green	Jiu Hang
Tea-7	Japan	Kyushu	Green	Yabukita
Tea-8	Japan	Kyushu	Green	Yabukita
Tea-9	China	Jiangsu	Black	Xiao Ye
Tea-10	China	Jiangsu	Black	Xiao Ye
Tea-11	China	Jiangsu	Black	Xiao Ye
Tea-12	India	Darjeeling	Black	China Jat (Mix)
Tea-13	India	Darjeeling	Black	China Jat (Mix)
Tea-14	India	Darjeeling	Black	China Jat (Mix)
Tea-15	China	Taiwan Ali mountain	Black	Chin Shin
Tea-16	China	Taiwan Ali mountain	Oolong	Chin Shin
Tea-17	Vietnam	Lai Chau	Oolong	Jin Xuan
Tea-18	Vietnam	Lai Chau	Oolong	Jin Xuan
Tea-19	Vietnam	Lai Chau	White	Jin Xuan
Tea-20	Vietnam	Lai Chau	Black	Jin Xuan
Tea-21	Vietnam	Lao Cai	Green	Da Ye age
Tea-22	China	Yunnan	Dark	Da Ye
Tea-23	China	Yunnan	Dark	Da Ye
Tea-24	China	Yunnan	Dark	Da Ye
Tea-25	Sri Lanka	Ratnapura	Black	Assamica

Tea-26	Sri Lanka	Matara	Black	Assamica
--------	-----------	--------	-------	----------

126

127 *Table 1: Tea samples description*

128 2.2. Inorganic signature of tea

129 Three grams of tea were dry ground using a porcelain mortar. The obtained powder was transferred  
 130 to a zipped polyethylene bag (Nalgene, Thermo Fisher Scientific, Illkirch-Graffenstaden, France) and  
 131 stored in a dry, dark place until analysis. The tea powder (0.2–0.4 g) was combined with 7 mL of sub-  
 132 boiled nitric acid (HNO<sub>3</sub>; 69.0%–70.0%, Instra Analysed Reagent, J.T.Baker®, Fisher Scientific, France)  
 133 and left to react overnight at room temperature. Then, 1 mL of hydrogen peroxide (H<sub>2</sub>O<sub>2</sub>; 30%,  
 134 ULTREX® II Ultrapure Reagent, J.T.Baker®, Thermo Fisher Scientific, Illkirch-Graffenstaden, France) was  
 135 added to the sample–acid solution. The final mixture was then digested in a microwave system  
 136 (Ultrawave SRC technology, Milestones, Sorisole (BG), Italy) following an optimized gradual heating  
 137 program up to 250° C, where the temperature was maintained for 20 min at P max = 110 bar. An  
 138 aliquot of the resulting clear solutions was then used for multi-elemental analysis, and the rest of  
 139 mineralized solution was transferred to clean PFA vials (Savillex Corporation, Eden Prairie, MN, USA).

140

141 2.2.1. Multielemental composition determination using quadrupole ICP-MS

142 Aliquots of diluted solutions were used for multielement analysis of tea samples using an ICP-MS  
 143 Plasma Quant Elite spectrometer (Analytik Jena, Jena, Germany). All the samples were analysed to  
 144 determine the total concentration levels of 21 elements: Al, As, B, Ba, Ca, Cd, Co, Cr, Cu, Fe, K, Li, Mg,  
 145 Mn, Na, Ni, Rb, Sr, Pb, V, and Zn. Instrument operating conditions and measured isotopes are  
 146 presented in Table SI2. The analysis was performed using two operating modes: a standard "no gas"  
 147 mode and an integrated collisional reaction cell (iCRC) mode. Helium (He) and hydrogen (H<sub>2</sub>) (Air  
 148 Liquide, Paris, France) were used as collision and reaction gases, respectively, to reduce spectral  
 149 interference. For the external calibration, solutions were prepared at eight concentration levels,  
 150 ranging from 0.01 to 500 µg L<sup>-1</sup>, via an appropriate dilution of the multielement standard solutions,  
 151 CCS-4 and CCS-6 (Inorganic ventures, Christiansburg, VA, USA). Yttrium, rhodium, and iridium at the  
 152 concentrations of 2.5 µg L<sup>-1</sup> were used as internal standards for the low, medium, and heavy masses,  
 153 respectively, to correct instrumental drifts. Sample concentrations were calculated after applying the  
 154 corrections for the analytical and procedural blanks as well as internal standards. Accuracy and  
 155 precision of the measurements were controlled by analysing the following certified reference  
 156 materials: NIST SRM 1643f (trace elements in water, The National Institute of Standards and  
 157 Technology, Gaithersburg, MD, USA) and CRM NIES 23 (National Institute for Environmental Studies,  
 158 Tsukuba-City, Ibaraki, Japan). Recoveries were within the acceptable limit of ±10%.

159 2.2.2. Sr Isotope analysis using the Multi-collector MC-ICP-MS

160 An appropriate volume of each digested solution sample was evaporated to dryness to obtain 4 µg of  
 161 Sr. The residue was then dissolved in 3M HNO<sub>3</sub>. Subsequently, Sr was separated from the matrix using  
 162 columns containing Eichrom Sr-Spec resin (Eichrom Technologies Inc, Lisle, USA) via sequential elution  
 163 with ultrapure water and 3M ultrapure HNO<sub>3</sub>, as previously described by Martin *et al.*. Sr isotope  
 164 analysis was performed using a Nu Plasma MC-ICP-MS (Nu Instruments, Wrexham, UK) with wet  
 165 plasma conditions and a self-aspirating micro concentric nebulizer (200 µL min<sup>-1</sup>) combined with a  
 166 glass cyclonic spray chamber. Measurements were performed using a conventional "Sample–  
 167 Standard–Bracketing" calibration sequence with SRM 987 (Sr carbonate isotopic standard, NIST,

168 Gaithersburg, MD, United States) used as a bracketing standard after every two samples. After  
169 instrumental blank subtraction using the on-peak-zero approach, the  $^{87}\text{Sr}/^{86}\text{Sr}$  ratios were corrected  
170 for instrument mass bias through an exponential law with a constant  $^{86}\text{Sr}/^{88}\text{Sr}$  ratio of 0.1194 and for  
171 the potential remaining interferences from the traces of  $^{87}\text{Rb}$  using the monitored  $^{85}\text{Rb}$  and a  $^{85}\text{Rb}/^{87}\text{Rb}$   
172 ratio of 2.5926. The value of  $^{87}\text{Sr}/^{86}\text{Sr}$  ratio was 0.710255 for SRM 987 applied for data processing,  
173 according to Waight *et al.*.

174 The  $^{87}\text{Sr}/^{86}\text{Sr}$  ratio was normalized to the certified reference material NIST CRM 987 according to the  
175 following equation (Liu *et al.*, 2014):

$$176 \quad \delta^{87}\text{Sr} = \left[ \frac{(^{87}\text{Sr}/^{86}\text{Sr})_{\text{sample}}}{(^{87}\text{Sr}/^{86}\text{Sr})_{\text{NIST987}}} - 1 \right] \times 1000(\text{‰}).$$

177 *Equation 1*

### 178 2.3. Analysis of volatile components with SIFT-MS

179 SIFT-MS measurements were performed on headspace contents of tea samples. Ten grams of tea were  
180 introduced into a 1-L glass bottle (Schott, Colombes, France) fitted with a polypropylene screw cap  
181 with two tight connection ports fitted (Duran Wheaton Kimble, Holzminden, Germany) with 0.6-cm  
182 PFA tubes (Swagelock, Lyon, France). The first tube was connected directly to the SIFT-MS and the  
183 second to a 1-L Tedlar© bag (Supelco, Bellefonte, PA, USA), filled with zero dry air (ZeroAir Alliance  
184 ZA1500, F-DGSi, Evry, France). This bag compensated for analysed volume during SIFT-MS analyses.  
185 The closed bottle was incubated for 2 hours at 60°C to achieve equilibrium in the gas phase before  
186 performing the positive and negative SIFT-MS full scan analysis.

187 A SIFT-MS Voice 200 Ultra (SYFT Technologies, Christchurch, New Zealand) instrument equipped with  
188 a dual source producing positive and negative soft ionizing precursor ions ( $\text{H}_3\text{O}^+$ ,  $\text{O}_2^{\bullet+}$ ,  $\text{NO}^+$ ,  $\text{O}^{\bullet-}$ ,  $\text{OH}^-$ ,  
189  $\text{O}_2^{\bullet-}$ ,  $\text{NO}_2^-$  and  $\text{NO}_3^-$ ) was used in a single scan. This instrument used nitrogen (Air Liquide, Alphagaz 2,  
190 Paris, France) as the carrier gas; the sample was introduced through a heated (110°C) and flow-  
191 controlled ( $20 \text{ mL min}^{-1}$ ) sample line (High-Performance Inlet HPI®, SYFT Technology, Christchurch,  
192 New Zealand). The instrument was calibrated daily using a standard gas (Scott™ gas mixtures, Air  
193 Liquid, Breda, Netherlands), containing standards at 2.0 ppmV in nitrogen. A blank experiment was  
194 performed for each empty bottle before analysing all of them in triplicate. The full scan raw data files  
195 containing product ion intensities in the 15–250 m/z range were collected before compilation and pre-  
196 processing steps.

197 Compilation and pre-processing of the full scan raw data were performed as described in a previous  
198 study (Reyrolle *et al.*, 2022) using Python language. Data was pre-processed by subtracting background  
199 noise (signal of bottles without samples) for each replicate. Triplicates of each sample were averaged  
200 to obtain a single value of signal intensity for each ion. This value was multiplied by the ICF factor  
201 corresponding to the instrument calibration correction. The dataset was cleaned by suppressing  
202 constant quantitative variables.

203

### 204 2.4. Statistical analysis

205 Statistical analysis, including non-supervised and supervised methods, was performed using the R  
206 language and MixOmics package (Rohart *et al.*, 2017). Multielement analysis and Sr isotope data were  
207 evaluated via principal component and partial least-squares-discriminant analyses. For volatile  
208 fingerprint analysis, sparse principal component analyses (Sparse PCA) and sparse partial least-squares  
209 discriminant analyses (sPLS-DA) were used to show the dispersion or discrimination of the sample

210 based on many variables. Inorganic elemental contents and  $^{87}\text{Sr}/^{86}\text{Sr}$  ratios were combined by  
211 normalizing the latter was normalized to the certified reference material NIST CRM 987 ( $\delta^{87}\text{Sr}_{\text{NIST987}}$ )  
212 using equation 1.

213

---

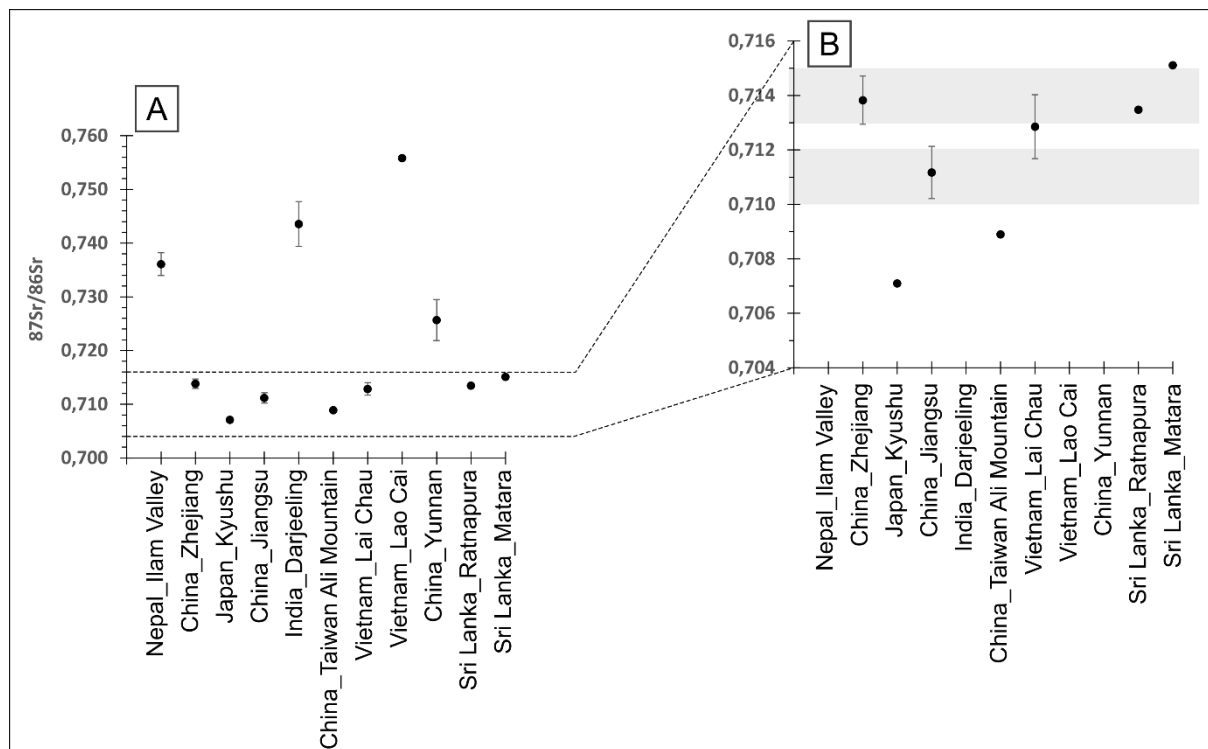
### 214 3. Results & Discussion

#### 215 3.1. inorganic signatures

216 Studies on geographical origin of food products that use multiple markers (trace element fingerprints,  
217 stable isotope signatures) have been steadily increasing over recent years (Bandoniene et al., 2018).  
218 Trace element fingerprints can be used to determine origin of products, especially for plants in which  
219 the primary element composition is derived from the bioavailable fraction of elements in soil (Bataille  
220 et al., 2020). Sr isotopes, radiogenic  $^{87}\text{Sr}$  vs. stable  $^{86}\text{Sr}$  ( $^{87}\text{Sr}/^{86}\text{Sr}$ ), were primarily used to infer  
221 geographical provenance and thus were often applied in fisheries or food sciences (Epova et al., 2019).  
222 The  $^{87}\text{Sr}/^{86}\text{Sr}$  ratio has several advantages. First of all, Sr is absorbed into biological materials in a  
223 conservative manner, i.e., without biological fractionation across the food chain. Secondly, the Sr  
224 isotope ratio mainly depends on the bioavailable Sr in soil, a fraction largely controlled by differential  
225 weathering of minerals from parent bedrock and soil with varying Sr and Rb concentrations (Rb/Sr  
226 ratio). Ultimately, the combination of lithology, weathering, and additional Sr sources (atmospheric  
227 and anthropogenic) produces considerable variability in available  $^{87}\text{Sr}/^{86}\text{Sr}$  ratios in the geosphere and  
228 thus the biosphere (Bataille et al., 2020).

229 The  $^{87}\text{Sr}/^{86}\text{Sr}$  ratios in tea samples clearly discriminated six regions (China\_Yunnan, India\_Darjeeling,  
230 Nepal\_Ilam Valley, Vietnam\_Lao Cai, China\_Taiwan Ali Mountain, and Japan\_Kyushu) from 11  
231 collection sites (figure 1), confirming the success of this technique to determine geographical origin,  
232 as previously mentioned in the scientific literature. Globally,  $^{87}\text{Sr}/^{86}\text{Sr}$  ratios found in our tea samples  
233 were consistent with those reported in recent provenance studies (Aoyama et al., 2017; X. Wang &  
234 Tang, 2020), strengthening the link between plants and bioavailable  $^{87}\text{Sr}/^{86}\text{Sr}$  ratios (Bataille et al.,  
235 2020). Our high  $^{87}\text{Sr}/^{86}\text{Sr}$  ratios for Darjeeling tea (average =  $0.744 \pm 0.004$  and  $n = 3$ ) correspond to  
236 those published for the same region (Lagad et al., 2013) (average =  $0.745 \pm 0.029$ , range =  $0.726\text{--}0.829$ ,  
237 and  $n = 9$ ) but with a lower dispersion. The wide range of variation in  $^{87}\text{Sr}/^{86}\text{Sr}$  ratios reported by Lagad  
238 et al is consistent with ratios in local water and soils developed from granitic to gneissic rocks (Galy et  
239 al., 1999). The narrow range in  $^{87}\text{Sr}/^{86}\text{Sr}$  ratios we observed is due to the unique geographical origin of  
240 our three samples. Our analyses did not discriminate however the Darjeeling region from the Ilam  
241 Valley (Nepal =  $0.736 \pm 0.002$  and  $n = 3$ ) or Lao Cai (Vietnam =  $0.7558$  and  $n = 1$ ). The combination of  
242  $^{87}\text{Sr}/^{86}\text{Sr}$  ratios and trace element concentrations of Ca, Sr, Ba, Cd, and K allowed such discriminations  
243 (figure 2). Moreover, Vietnam\_Lao Cai teas were enriched in Rb and Fe compared to India\_Darjeeling  
244 teas providing more reliability in the separation of these sources. A geographical association was  
245 assigned by the “Tea Board India” to protect Darjeeling tea and preserve iconic stature in India's  
246 cultural heritage. Thus, a combination of Sr isotope ratios and trace elements may demonstrate the  
247 authenticity of the product and highlight fake products labelled as “Darjeeling tea.” Finally, the volcanic  
248 substratum of the Kyushu province in Japan shows a characteristic  $^{87}\text{Sr}/^{86}\text{Sr}$  ratio that set it apart from  
249 other sources worldwide (Aoyama et al., 2017). An additional factor in distinguishing these teas is the  
250 relatively large levels of Na that complete Sr isotope ratios.



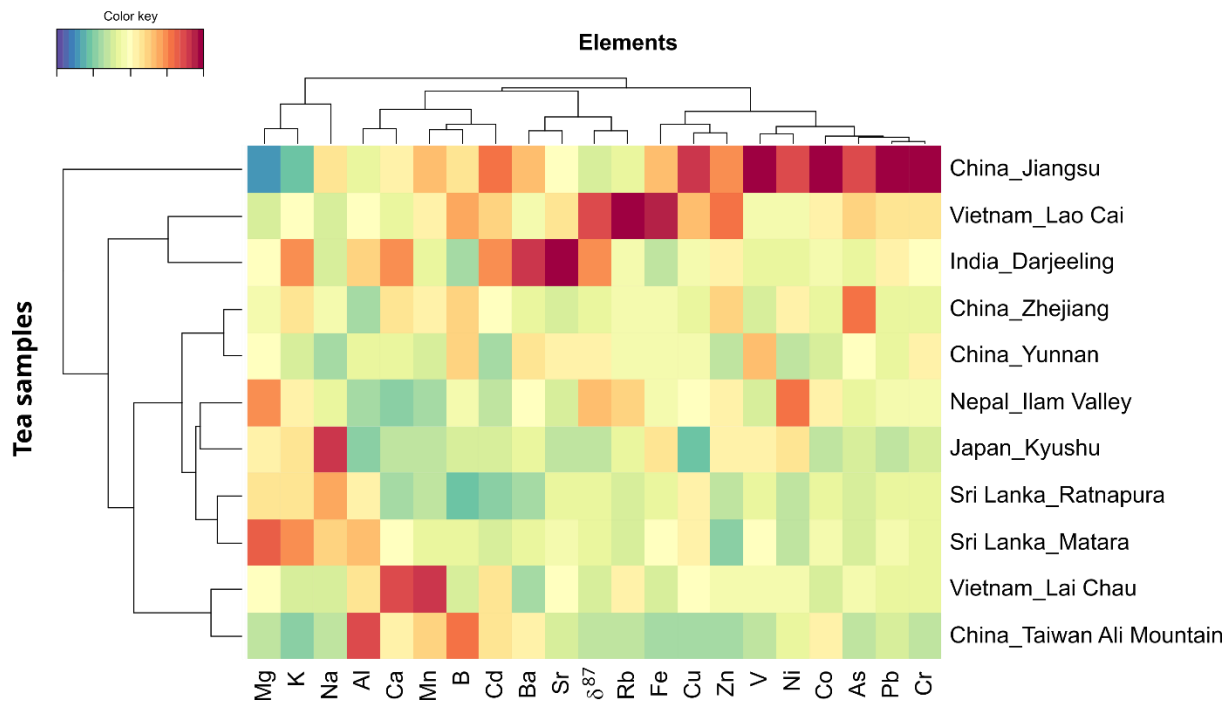


251  
 252 Figure 1: Sr isotope ratios ( $^{87}\text{Sr}/^{86}\text{Sr}$ ) according to the regions. The mean values are represented with circles and the standard  
 253 deviation with vertical lines. Figure 1B represents a zoom of figure 1A between 0.704 and 0.716 of  $^{87}\text{Sr}/^{86}\text{Sr}$

254

255  $^{87}\text{Sr}/^{86}\text{Sr}$  ratios appeared to overlap between the following sites, Sri Lanka\_Ratnapura and  
 256 Sri\_lanka\_Matara, Vietnam\_Lai Chau, and China\_Zhejiang, on the one hand, and China\_Jiangsu and  
 257 Vietnam\_Lai Chau, on the other. Nonetheless, we identified inorganic profiles among these sites that  
 258 allowed differentiation. Similarities and differences in chemical fingerprints of teas were assessed  
 259 across sites and countries of origin using a partial least square regression and a discriminant analysis  
 260 to create a hierarchical clustering heatmap (Figure 2). Elemental concentrations and  $\delta^{87}\text{Sr}$  are  
 261 presented as variables (in columns), and regions and countries of origin are presented as observations  
 262 (in rows). The two Sri Lankan sites were an exception. For instance, China\_Jiangsu teas presented high  
 263 levels of V, Co, Cr, Pb, and Cu compared to four other sites and those already discriminated using Sr  
 264 isotope ratios. Higher concentrations are associated with surrounding mines and industrial activities.  
 265 More specifically, elemental profiles in heavy metals were related to the presence of 12 mines, listed  
 266 by the United States Geological Survey, that produce Fe, Cu, Zn, Pb, Cr, V, and Ag. Moreover, GEM,  
 267 one of the largest battery recyclers in China that processes used battery and produces 10,000 tons of  
 268 cobalt tetroxide in Jiangsu. These elements were, therefore, good markers of anthropogenic impact  
 269 on multielement signatures and allow the identification of teas from this region. Furthermore,  
 270 China\_Zhejiang, Vietnam\_Lai Chau, and Sri Lanka\_Ratnapura/Matara teas differed in As  
 271 concentrations and Ca/Mn and Na/Mg ratios, respectively. Our results confirmed that multielement  
 272 signatures are useful indicators, especially for tea authentication, since they reflect climate,  
 273 environment, and agricultural practices (Camin et al., 2017). Finally, combining Sr isotope ratios and  
 274 elemental fingerprints enabled to distinguish 10 out of 11 tea samples with a significance level of 0.05.  
 275 Nine origins displayed unique geochemical signatures, i.e., China\_Jiangsu, Vietnam\_Lao Cai,  
 276 India\_Darjeeling, Nepal\_Ilam Valley, Japan\_Kyushu, Vietnam\_Lai Chau, China\_Taiwan Ali Mountain,  
 277 China\_Zhejiang, and China\_Yunnan, along with one group of two sites (two Sri Lanka provinces:  
 278 Ratnapura and Matara districts). Four sites or groups of sites were primarily discriminated according

279 to their elemental content (China\_Jiangsu, Sri Lanka\_Ratnapura/Matara, Vietnam\_Lai Chau, and  
 280 China\_Zhejiang), three sites mainly by their  $^{87}\text{Sr}/^{86}\text{Sr}$  ratio (Nepal\_Ilam Valley, China\_Yunnan, and  
 281 China\_Taiwan Ali Mountain), and three sites according to the  $^{87}\text{Sr}/^{86}\text{Sr}$  ratio ( $\delta^{87}\text{Sr}$ ) as well as specific  
 282 elemental concentrations (Vietnam\_Lao Cai, India\_Darjeeling, and Japan\_Kyushu) (Figure 2 and Table  
 283 S12).



284  
 285 Figure 2: A clustered image map (CIM) based on PLS-DA and according to the “country\_region of origin” parameter. The  
 286 dendrograms represent hierarchical grouping for regions (horizontal) and for elements (vertical). The colour key indicates the  
 287 under expression (in blue scale) or over expression (in red scale) of the element in each sample group in relation to the others.

288

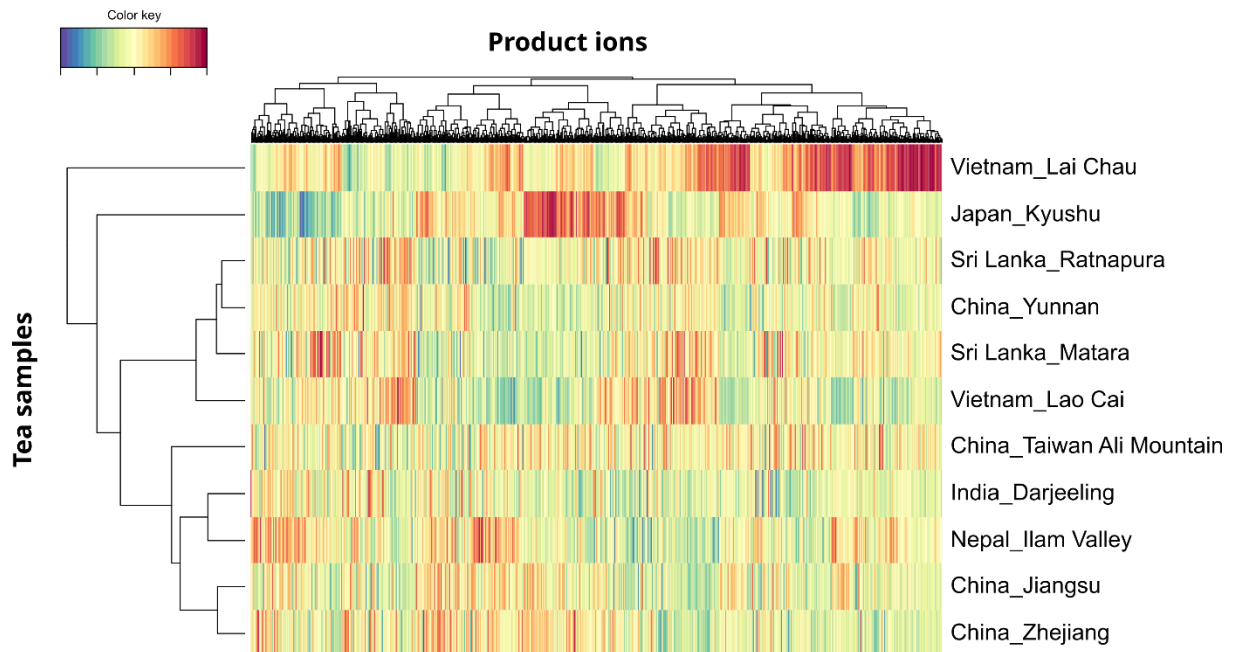
### 289 3.2. Volatile fingerprints

290 VOCs released from food products have been studied for many years. VOCs are good markers of plant,  
 291 animal, and microbial metabolisms involved in food production and transformation. Taste and aroma  
 292 are generally sufficient to identify specific compounds because of the high complexity of human  
 293 perception. New approaches, based on nonspecific analysis of food combined with statistical tools,  
 294 allow use of correlations between qualitative attributes and chemical composition. Direct injection  
 295 mass spectrometers, such as PTR-MS and SIFT-MS, are powerful instruments for investigating VOCs,  
 296 thanks to their high chemical selectivity. Thus, specific biogenesis of volatile molecules in plants, such  
 297 as olive oil (Ozcan-Sinir, 2020) or saffron (Nenadis et al., 2016), can be used to control processes, such  
 298 as drying (Olivares et al., 2011), roasting (Dryahina et al., 2018), oxidation and fermentation (Van  
 299 Kerrebroeck et al., 2015). Analyses can also be used to demonstrate typical profiles for dark chocolates  
 300 and ewe cheeses (Deuscher et al., 2019; Reyrolle et al., 2022). Traceability of food products can be, in  
 301 some cases, correlated with taste and flavour but it requires highly experienced experts. In this work,  
 302 static headspaces of tea samples were analysed with SIFT-MS Voice 200-ultra creating volatile  
 303 fingerprints with 1,880 variables by combining the raw signals in a full scan mode (15-250 m/z)  
 304 obtained with the three positive precursor ions and the five negative precursor ions.

305

306 3.2.1. Unsupervised analysis of tea samples grouped by the region of origin

307 The power of the volatile fingerprint approach lies in the search for correlation of VOCs signals with  
308 descriptive values. An unsupervised sparse principal component analysis (sparse PCA) was performed  
309 on the volatile fingerprints obtained from 26 tea samples (mean of triplicates) by grouping them by  
310 region of origin and then representing them on the cluster image map (Figure 3).



311  
312 Figure 3: A clustered image map (CIM) based on Sparse PCA analysis of volatile compound fingerprints according to the  
313 parameter "country\_region of origin". The horizontal dendrogram represents the hierarchical grouping per tea region and  
314 the vertical dendrogram for product ions. The colour key indicates the under expression (in blue scale) or overexpression (in  
315 red scale) of the product ion in each group sample in relation to the other samples.

316 No obvious classification of tea samples according to the country was observed (i.e., Chinese,  
317 Vietnamese, and Sri Lankan samples were not grouped). Vietnam\_Lai Chau showed a completely  
318 different pattern to the rest of the dataset, with a large number of product ions overexpressed  
319 compared to the entire dataset. Surprisingly, this profile corresponds to the average of four different  
320 samples with different processes (oolong tea = 2, white tea = 1, and black tea = 1). Japan\_Kyushu tea,  
321 presented another cluster of product ions that were overexpressed compared to the entire dataset  
322 and that separated these samples from the rest of the collection. Despite the lack of classification by  
323 country, the product knowledge allowed us to further interpret this cluster image.

324 Indeed, apart from these two origins with very different volatile profiles, the other samples seem to  
325 be classified in 2 clusters. A first cluster of region profiles included Sri Lanka\_Ratnapura, Sri  
326 Lanka\_Matara, China\_Yunnan, and Vietnam\_Lao Cai samples. The similarity of volatile fingerprints for  
327 these four regions cannot be explained by geographical proximity. However, this didn't come over  
328 surprised to our tea expert because the two cultivars grown in these four provinces are both large-  
329 leafed teas.

330 In the second cluster, the volatile fingerprints of tea samples from China\_Zhejiang and China\_Jiangsu  
331 were similar, which can be explained by the geographical proximity of the two production areas and  
332 the use of similar cultivars (Jiu Hang and Xiao Ye), small-leafed *C. sinensis var sinensis* tea bushes.  
333 Following the same trend, the volatile fingerprints of India\_Darjeeling and Nepal\_Ilam Valley teas were  
334 similar due to the geographical proximity of the two production areas and the use of a similar mix of

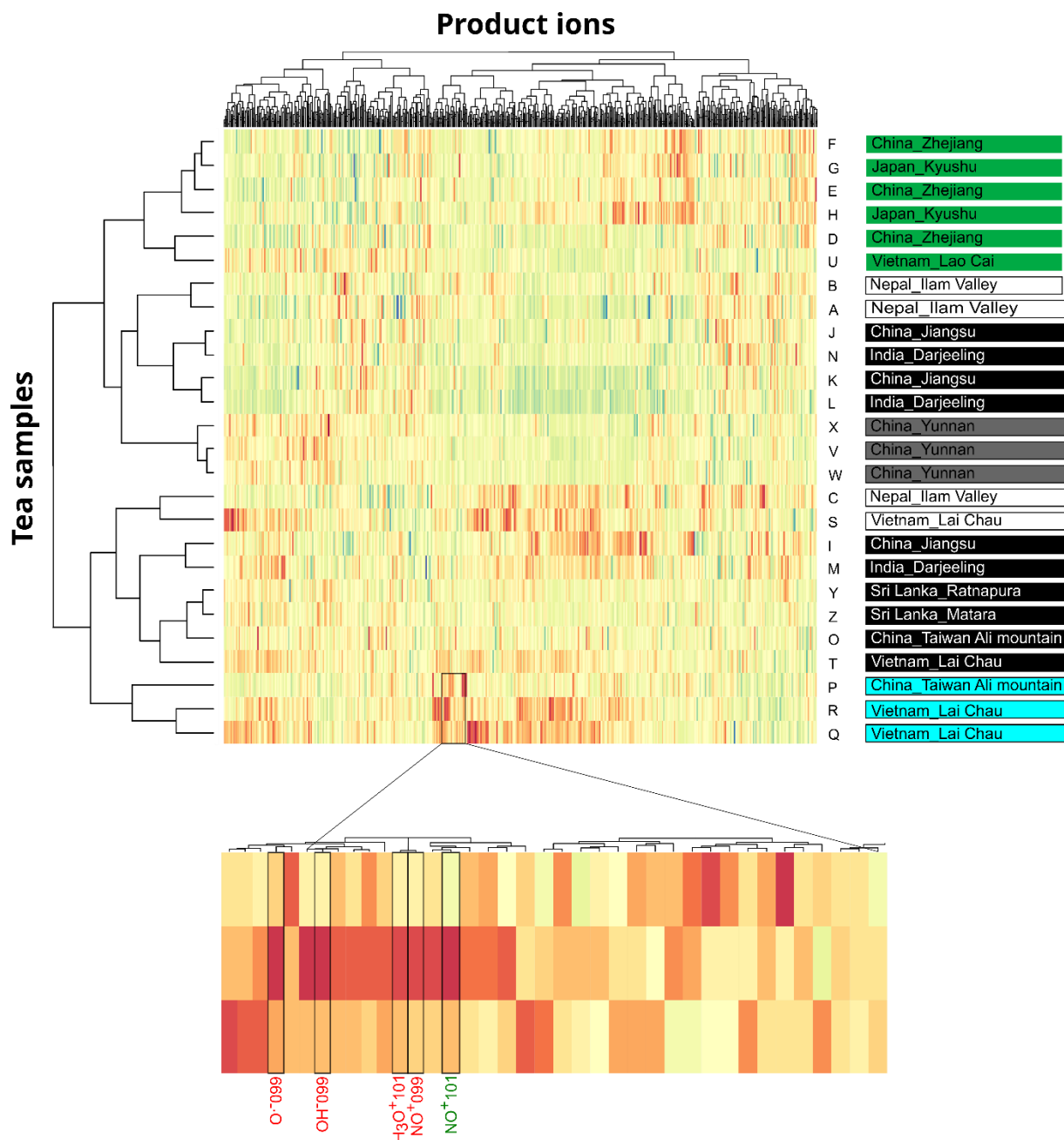
335 cultivars: a mixture of small-leaf teas from eastern China and *assamica* (large-leaf tea). The similarity  
336 of volatile fingerprints between the Darjeeling and Ilam Valley tea samples and those from Jiangsu and  
337 Zhejiang could be explain by the same cultivar base (small-leaf tea). The small-leaf tea plants in the  
338 mix of cultivars seem to contribute more to the typicality of the Darjeeling and Ilam Valley tea  
339 characteristics in a clone mix compared to the large-leaf tea plants.

340 The profiles of Japanese teas are consistent with a specific unique terroir, and also because Japanese  
341 research institutes have developed a new variety of *C. sinensis*, *Yabukita*, adapted to their climatic  
342 conditions. Teas from Vietnam\_Lai Chau province are produced from a tea plant called *Jin Xuan*  
343 developed in Taiwan by the Tea Research and Extension Station and subsequently imported to this  
344 region. We were expecting similar volatile fingerprints between these two regions, Vietnam\_Lai Chau  
345 and China\_Taiwan Ali mountain however this was not the case. Therefore, this may suggest that  
346 growing areas also play a role in inducing differences between regions. The secret of the genetic  
347 selection of tea cultivars combined with the number of cultivars makes the understanding of  
348 phylogenetic relationships complex. The use of different cultivars in the two Vietnamese provinces  
349 notably affects volatile profiles (Figure 4).

350

### 351 3.2.2.Volatile fingerprints obtained from processing methods

352 Our partner collected samples directly from producers in different countries, thus recovering samples  
353 of various origins and colours, corresponding to the tea leaves transformation processes. Using colour  
354 labels of the tea principal component analysis does not enable to group tea together based on  
355 processing method, which therefore suggested that the process is not the predominant factor in the  
356 volatile footprint of tea. Then, a supervised analysis (sparse PLS-DA) was performed on the volatile  
357 fingerprints of the 26 tea samples to highlight the impact of transformation processes which can be  
358 seen on the cluster image map (Figure 4). This statistical tool allowed the identification of  
359 commonalities among volatile fingerprints and differences between classes. The dendrogram on the  
360 left of the map corresponds to the classification of tea based on volatile profiles, and the dendrogram  
361 at the top corresponds to the classification of product ions.



362

363 Figure 4: Clustered image maps (CIM) based on sparse PLS-DA analysis of volatile compound fingerprints based on  
 364 colour/processing of tea. Green teas were highlighted with green, Oolong teas with blue, black teas highlighted with black,  
 365 Dark teas highlighted with grey and white teas highlighted with white. The dendrograms represent hierarchical grouping for  
 366 tea samples (horizontal) and for product ions (vertical). The colour key indicates the under expression (in blue scale) or  
 367 overexpression (in red scale) of the product ion in each group sample compared to the other samples. A zoom was drawn to  
 368 highlight the position of the different product ions coming from hexanal (red) and hexanol (green)

369

370

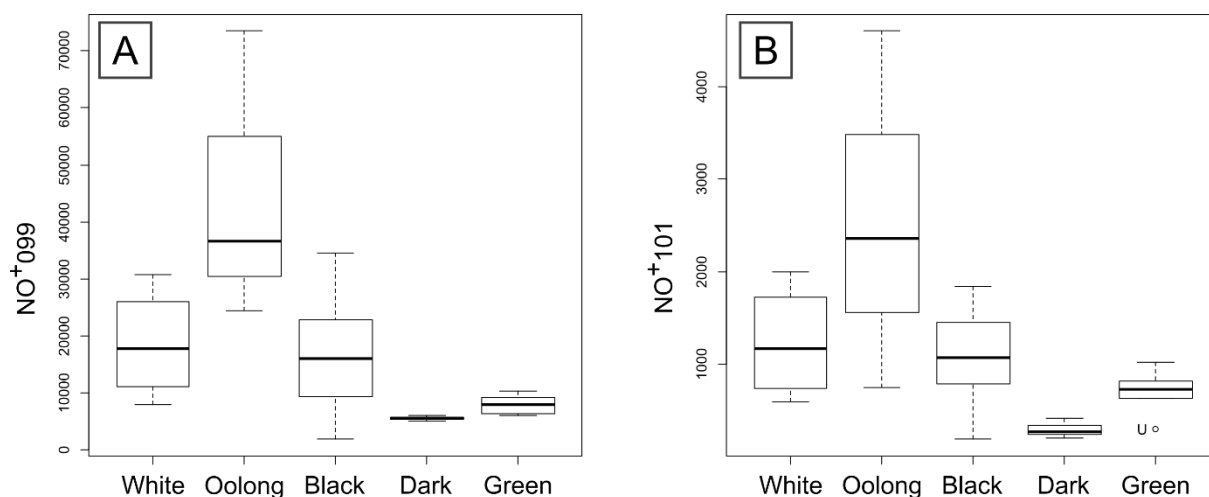
371 The supervised analysis of volatile fingerprints based on the dataset according to the colours of teas  
 372 shows a good discrimination of green and oolong teas (Figure 4). The green teas were all grouped  
 373 together and were furthest away from the oolong tea cluster. Green teas are not oxidised, whereas  
 374 oolong teas are (Feng et al., 2019; Zhang et al., 2019). Recent studies observed that Oolong tea  
 375 produced from several cultivars presented significantly different aroma profiles (Guo et al., 2022; Tan  
 376 et al., 2022). We observed a quite high statistical distance between oolong teas with cultivar Chin Shin

377 from China\_Taiwan Ali mountain and oolong teas with cultivar Jin Xuan from Vietnam\_Lai Chau. But,  
378 in our sample set, these three Oolong teas were clearly grouped together and separated from the  
379 other colours.

380 A third cluster of dark teas from China\_Yunnan province was observed at the center of the cluster  
381 image map, with short statistical distance, indicating a strong similarity in their volatile fingerprints.  
382 These teas are also called “Pu Erh,” and correspond to post-fermented teas. (Zhang et al., 2013).

383 Black and white teas were mixed into two groups; some shared features with the oolong group and  
384 others with the dark group. In our dataset, volatile fingerprints did not clearly discriminate black and  
385 white teas into two separated clusters. Black tea is produced in large quantities with various process  
386 stages allowing different degrees of oxidation and roasting (Alasalvar et al., 2012). Finally, white tea is  
387 the least known, produced from buds or young leaves with a process of prolonged withering,  
388 allowing slight enzymatic oxidation and drying (Chen et al., 2019; Dai et al., 2017). Black and white teas  
389 were not discriminated using SIFT-MS. The worldwide diversity of cultivars, agricultural practices, and  
390 processing techniques produce several types of tea. Some of them were easy to identify (green, dark  
391 and oolong), whereas the other had too high level of similarity in term of VOCs to be grouped using  
392 this approach.

393 Volatile fingerprints allowed discrimination among dark (fermented), oolong (oxidized), and green (not  
394 oxidized) teas, which are very different. The plot Loadings figure (SI3) showed the 40 most  
395 discriminating product ions on the first component of the sPLS-DA. Unitary mass resolution of the  
396 instrument and possible ion conflicts affected the identification of molecules within the list.  
397 Nevertheless, five product ions corresponding to hexanal displayed positive discrimination for oolong  
398 teas ( $H_3O^+$  m/z 101,  $NO^+$  m/z 99,  $O^-$  m/z 99,  $O_2^-$  m/z 99, and  $OH^-$  m/z 99). These particular teas are  
399 oxidised with higher levels of oxygenated molecules, such as aldehydes or alcohols among which  
400 hexanal and hexanol were previously identified (Zhou et al., 2020). The boxplot (Figure 5) shows the  
401 intensity of one ion produced by hexanal ( $NO^+$  m/z 99) and by hexanol ( $NO^+$  m/z 101) in different tea  
402 categories. Weaker signals were observed for green and dark teas that were consistent due to the lack  
403 of oxidation, and the strongest signals were observed for oolong teas. Black and white teas displayed  
404 intermediate levels for these product ions.



405  
406 *Figure 5: Boxplot of the intensity of product ions X3099 ( $NO^+$  m/z 99) corresponding to hexanal (A) and X3101 ( $NO^+$  m/z 101)*  
407 *corresponding to hexanol (B) for each colour of tea.*

## 408 4. Conclusion

409

410 This work showed for the first time that the combination of volatile fingerprints with inorganic  
411 signatures can greatly improve the authentication of tea.  $^{87}\text{Sr}/^{86}\text{Sr}$  ratio reflecting the bioavailable  
412 fraction of Sr derived from the mineral weathering processes of bedrock and soil was a well-known  
413 marker of geographical origin. It was demonstrated that completing this signature with elemental  
414 composition increased the ability to discriminate the 11 production regions of the studied tea  
415 samples (from 6 using only  $^{87}\text{Sr}/^{86}\text{Sr}$  ratio to 10). Only the two locations in Sri Lanka seemed to  
416 share a common inorganic pattern. The origin of a food product is nevertheless not sufficient to  
417 ensure its conformity. For centuries, varietal selection of *Camelia sinensis* has led to a large number  
418 of cultivars that have developed their own aroma and cultivation properties. It is therefore very  
419 important for an authentic tea to be produced from the right cultivar that has undergone the  
420 appropriate processing steps. It was demonstrated that the main contributing factor of tea volatile  
421 fingerprints recorded with SIFT-MS was the type of cultivar. In a second approach, with a  
422 supervised statistical analysis, the different colours of tea reflecting different rates of oxidation  
423 were also separated. Oolong teas which are oxidized teas were clearly separated from the green  
424 ones, that are the least transformed teas and from dark / Pu Er samples which are fermented teas.  
425 We were not able to separate black and white teas because of the median level of oxidation of  
426 these types of tea and the variability of the different processes. Despite the technical limitations  
427 of the SIFT-MS instrument, i.e. its unit mass resolution and the presence of conflict ions, it was  
428 possible to show that the expression levels of the two molecules hexanal and hexanol were  
429 consistent with oxidation level. The statistical proximity of the ions corresponding to these two  
430 molecules in the vertical cluster means that these signals vary similarly in our dataset and may  
431 correspond to a metabolic pathway. The present study emphasizes the potential of combining  
432 instrumental and chemometric analyses to improve the traceability of teas and can also help to  
433 ensure product quality and safety throughout the food industry sectors. The application of the  
434 proposed analytical strategy on a collection of tea samples adapted in number and quality will  
435 enable the construction of a predictive model to answer questions related to product traceability  
436 and authenticity.

### 437 **Funding and acknowledgments**

438 The Authors thank Conseil Régional Nouvelle Aquitaine (CRNA) for their financial support (Number  
439 2019EMVOL). A special thank to Olivier Donard for his valuable advice.

### 440 **Declaration of Competing Interest**

441 The authors declare that they have no known competing financial interests or personal relationships  
442 that could have appeared to influence the work reported in this paper.

443 Alasalvar, C., Topal, B., Serpen, A., Bahar, B., Pelvan, E., & Gökmen, V. (2012). Flavor Characteristics  
444 of Seven Grades of Black Tea Produced in Turkey. *Journal of Agricultural and Food Chemistry*,  
445 60(25), 6323–6332. <https://doi.org/10.1021/jf301498p>

446 Aoyama, K., Nakano, T., Shin, K.-C., Izawa, A., & Morita, S. (2017). Variation of strontium stable  
447 isotope ratios and origins of strontium in Japanese vegetables and comparison with Chinese  
448 vegetables. *Food Chemistry*, 237, 1186–1195.  
449 <https://doi.org/10.1016/j.foodchem.2017.06.027>

450 Bandoniene, D., Meisel, T., Rachetti, A., & Walkner, C. (2018). A tool to assure the geographical origin  
451 of local food products (glasshouse tomatoes) using labeling with rare earth elements: A tool  
452 to assure the geographical origin of local food products. *Journal of the Science of Food and*  
453 *Agriculture*, 98(12), 4769–4777. <https://doi.org/10.1002/jsfa.9124>

454 Bataille, C. P., Crowley, B. E., Wooller, M. J., & Bowen, G. J. (2020). Advances in global bioavailable  
455 strontium isoscapes. *Palaeogeography, Palaeoclimatology, Palaeoecology*, 555, 109849.  
456 <https://doi.org/10.1016/j.palaeo.2020.109849>

457 Bin, L., Wang, C., Liu, Z., He, W., Zhao, D., Fang, Y., Li, Y., Zhang, Z., Chen, P., Liu, W., & Rogers, K. M.  
458 (2022). Geographical origin traceability of muskmelon from Xinjiang province using stable  
459 isotopes and multi-elements with chemometrics. *Journal of Food Composition and Analysis*,  
460 106, 104320. <https://doi.org/10.1016/j.jfca.2021.104320>

461 Camin, F., Boner, M., Bontempo, L., Fauhl-Hassek, C., Kelly, S. D., Riedl, J., & Rossmann, A. (2017).  
462 Stable isotope techniques for verifying the declared geographical origin of food in legal cases.  
463 *Trends in Food Science & Technology*, 61, 176–187.  
464 <https://doi.org/10.1016/j.tifs.2016.12.007>

465 Chen, Q., Zhu, Y., Dai, W., Lv, H., Mu, B., Li, P., Tan, J., Ni, D., & Lin, Z. (2019). Aroma formation and  
466 dynamic changes during white tea processing. *Food Chemistry*, 274, 915–924.  
467 <https://doi.org/10.1016/j.foodchem.2018.09.072>



468 Dai, W., Xie, D., Lu, M., Li, P., Lv, H., Yang, C., Peng, Q., Zhu, Y., Guo, L., Zhang, Y., Tan, J., & Lin, Z.  
469 (2017). Characterization of white tea metabolome: Comparison against green and black tea  
470 by a nontargeted metabolomics approach. *Food Research International*, *96*, 40–45.  
471 <https://doi.org/10.1016/j.foodres.2017.03.028>

472 Deuscher, Z., Andriot, I., Sémon, E., Repoux, M., Preys, S., Roger, J.-M., Boulanger, R., Labouré, H., &  
473 Le Quéré, J.-L. (2019). Volatile compounds profiling by using proton transfer reaction-time of  
474 flight-mass spectrometry (PTR-ToF-MS). The case study of dark chocolates organoleptic  
475 differences. *Journal of Mass Spectrometry*, *54*(1), 92–119. <https://doi.org/10.1002/jms.4317>

476 Dryahina, K., Smith, D., & Španěl, P. (2018). Quantification of volatile compounds released by roasted  
477 coffee by selected ion flow tube mass spectrometry. *Rapid Communications in Mass*  
478 *Spectrometry*, *32*(9), 739–750. <https://doi.org/10.1002/rcm.8095>

479 Epova, E. N., Bérail, S., Séby, F., Barre, J. P. G., Vacchina, V., Médina, B., Sarthou, L., & Donard, O. F. X.  
480 (2020). Potential of lead elemental and isotopic signatures for authenticity and geographical  
481 origin of Bordeaux wines. *Food Chemistry*, *303*, 125277.  
482 <https://doi.org/10.1016/j.foodchem.2019.125277>

483 Epova, E. N., Bérail, S., Séby, F., Vacchina, V., Bareille, G., Médina, B., Sarthou, L., & Donard, O. F. X.  
484 (2019). Strontium elemental and isotopic signatures of Bordeaux wines for authenticity and  
485 geographical origin assessment. *Food Chemistry*, *294*, 35–45.  
486 <https://doi.org/10.1016/j.foodchem.2019.04.068>

487 Feng, Z., Li, Y., Li, M., Wang, Y., Zhang, L., Wan, X., & Yang, X. (2019). Tea aroma formation from six  
488 model manufacturing processes. *Food Chemistry*, *285*, 347–354.  
489 <https://doi.org/10.1016/j.foodchem.2019.01.174>

490 Galy, A., France-Lanord, C., & Derry, L. A. (1999). The strontium isotopic budget of Himalayan rivers  
491 in Nepal and Bangladesh. *Geochimica et Cosmochimica Acta*, *63*(13–14), 1905–1925.  
492 [https://doi.org/10.1016/S0016-7037\(99\)00081-2](https://doi.org/10.1016/S0016-7037(99)00081-2)

493 Gomes, D. A. S., Alves, J. P. dos S., da Silva, E. G. P., Novaes, C. G., Silva, D. S., Aguiar, R. M., Araújo, S.  
494 A., dos Santos, A. C. L., & Bezerra, M. A. (2019). Evaluation of metal content in tea samples  
495 commercialized in sachets using multivariate data analysis techniques. *Microchemical*  
496 *Journal*, *151*, 104248. <https://doi.org/10.1016/j.microc.2019.104248>

497 Guo, X., Schwab, W., Ho, C.-T., Song, C., & Wan, X. (2022). Characterization of the aroma profiles of  
498 oolong tea made from three tea cultivars by both GC–MS and GC-IMS. *Food Chemistry*, *376*,  
499 131933. <https://doi.org/10.1016/j.foodchem.2021.131933>

500 Lagad, R. A., Alamelu, D., Laskar, A. H., Rai, V. K., Singh, S. K., & Aggarwal, S. K. (2013). Isotope  
501 signature study of the tea samples produced at four different regions in India. *Analytical*  
502 *Methods*, *5*(6), 1604. <https://doi.org/10.1039/c3ay26142e>

503 Li, C., Kang, X., Nie, J., Li, A., Farag, M. A., Liu, C., Rogers, K. M., Xiao, J., & Yuan, Y. (2023). Recent  
504 advances in Chinese food authentication and origin verification using isotope ratio mass  
505 spectrometry. *Food Chemistry*, *398*, 133896.  
506 <https://doi.org/10.1016/j.foodchem.2022.133896>

507

508 Lin, J., Zhang, P., Pan, Z., Xu, H., Luo, Y., & Wang, X. (2013). Discrimination of oolong tea (*Camellia*  
509 *sinensis*) varieties based on feature extraction and selection from aromatic profiles analysed  
510 by HS-SPME/GC–MS. *Food Chemistry*, *141*(1), 259–265.  
511 <https://doi.org/10.1016/j.foodchem.2013.02.128>

512 Liu, H.-C., You, C.-F., Chen, C.-Y., Liu, Y.-C., & Chung, M.-T. (2014). Geographic determination of  
513 coffee beans using multi-element analysis and isotope ratios of boron and strontium. *Food*  
514 *Chemistry*, *142*, 439–445. <https://doi.org/10.1016/j.foodchem.2013.07.082>

515 Liu, W., Chen, Y., Liao, R., Zhao, J., Yang, H., & Wang, F. (2021). Authentication of the geographical  
516 origin of Guizhou green tea using stable isotope and mineral element signatures combined  
517 with chemometric analysis. *Food Control*, *125*, 107954.  
518 <https://doi.org/10.1016/j.foodcont.2021.107954>

519 Luykx, D. M. A. M., & van Ruth, S. M. (2008). An overview of analytical methods for determining the  
520 geographical origin of food products. *Food Chemistry*, *107*(2), 897–911.  
521 <https://doi.org/10.1016/j.foodchem.2007.09.038>

522 Martin, J., Bareille, G., Berail, S., Pecheyran, C., Daverat, F., Bru, N., Tabouret, H., & Donard, O.  
523 (2013). Spatial and temporal variations in otolith chemistry and relationships with water  
524 chemistry: A useful tool to distinguish Atlantic salmon *Salmo salar* parr from different natal  
525 streams: Otolith chemistry of *Salmo salar*. *Journal of Fish Biology*, *82*(5), 1556–1581.  
526 <https://doi.org/10.1111/jfb.12089>

527 Nasr, E. G., Epova, E. N., de Diego, A., Souissi, R., Hammami, M., Abderrazak, H., & F. X. Donard, O.  
528 (2021). Trace Elements Analysis of Tunisian and European Extra Virgin Olive Oils by ICP-MS  
529 and Chemometrics for Geographical Discrimination. *Foods*, *11*(1), 82.  
530 <https://doi.org/10.3390/foods11010082>

531 Nenadis, N., Heenan, S., Tsimidou, M. Z., & Van Ruth, S. (2016). Applicability of PTR-MS in the quality  
532 control of saffron. *Food Chemistry*, *196*, 961–967.  
533 <https://doi.org/10.1016/j.foodchem.2015.10.032>

534 Ni, K., Wang, J., Zhang, Q., Yi, X., Ma, L., Shi, Y., & Ruan, J. (2018). Multi-element composition and  
535 isotopic signatures for the geographical origin discrimination of green tea in China: A case  
536 study of Xihu Longjing. *Journal of Food Composition and Analysis*, *67*, 104–109.  
537 <https://doi.org/10.1016/j.jfca.2018.01.005>

538 Olivares, A., Dryahina, K., Navarro, J. L., Smith, D., Španěl, P., & Flores, M. (2011). SPME-GC-MS  
539 versus Selected Ion Flow Tube Mass Spectrometry (SIFT-MS) Analyses for the Study of  
540 Volatile Compound Generation and Oxidation Status during Dry Fermented Sausage  
541 Processing. *Journal of Agricultural and Food Chemistry*, *59*(5), 1931–1938.  
542 <https://doi.org/10.1021/jf104281a>

543 Ozcan-Sinir, G. (2020). Detection of adulteration in extra virgin olive oil by selected ion flow tube  
544 mass spectrometry (SIFT-MS) and chemometrics. *Food Control*, *118*, 107433.  
545 <https://doi.org/10.1016/j.foodcont.2020.107433>

546 Reyrolle, M., Ghislain, M., Bru, N., Vallverdu, G., Pigot, T., Desauziers, V., & Le Behec, M. (2022).  
547 Volatile fingerprint of food products with untargeted SIFT-MS data coupled with mixOmics  
548 methods for profile discrimination: Application case on cheese. *Food Chemistry*, *369*, 130801.  
549 <https://doi.org/10.1016/j.foodchem.2021.130801>

550 Rohart, F., Gautier, B., Singh, A., & Lê Cao, K.-A. (2017). mixOmics: An R package for 'omics feature  
551 selection and multiple data integration. *PLOS Computational Biology*, *13*(11), e1005752.  
552 <https://doi.org/10.1371/journal.pcbi.1005752>

553 Shuai, M., Peng, C., Niu, H., Shao, D., Hou, R., & Cai, H. (2022). Recent techniques for the  
554 authentication of the geographical origin of tea leaves from *Camellia sinensis*: A review. *Food*  
555 *Chemistry*, *374*, 131713. <https://doi.org/10.1016/j.foodchem.2021.131713>

556

557 Tan, H. R., Chan, L. Y., Lee, H. H., Xu, Y.-Q., & Zhou, W. (2022). Rapid authentication of Chinese  
558 oolong teas using atmospheric solids analysis probe-mass spectrometry (ASAP-MS) combined  
559 with supervised pattern recognition models. *Food Control*, *134*, 108736.  
560 <https://doi.org/10.1016/j.foodcont.2021.108736>

561

562 Van Kerrebroeck, S., Vercaemmen, J., Wuyts, R., & De Vuyst, L. (2015). Selected Ion Flow Tube–Mass  
563 Spectrometry for Online Monitoring of Submerged Fermentations: A Case Study of  
564 Sourdough Fermentation. *Journal of Agricultural and Food Chemistry*, *63*(3), 829–835.  
565 <https://doi.org/10.1021/jf505111m>

566 Waight, T., Baker, J., & Peate, D. (2002). Sr isotope ratio measurements by double-focusing MC-  
567 ICPMS: Techniques, observations and pitfalls. *International Journal of Mass Spectrometry*,  
568 *221*(3), 229–244. [https://doi.org/10.1016/S1387-3806\(02\)01016-3](https://doi.org/10.1016/S1387-3806(02)01016-3)

569 Wang, X., & Tang, Z. (2020). The first large-scale bioavailable Sr isotope map of China and its  
570 implication for provenance studies. *Earth-Science Reviews*, 210, 103353.  
571 <https://doi.org/10.1016/j.earscirev.2020.103353>

572 Yener, S., Sánchez-López, J. A., Granitto, P. M., Cappellin, L., Märk, T. D., Zimmermann, R., Bonn, G.  
573 K., Yeretian, C., & Biasioli, F. (2016). Rapid and direct volatile compound profiling of black  
574 and green teas (*Camellia sinensis*) from different countries with PTR-ToF-MS. *Talanta*, 152,  
575 45–53. <https://doi.org/10.1016/j.talanta.2016.01.050>

576 Zhang, L., Ho, C., Zhou, J., Santos, J. S., Armstrong, L., & Granato, D. (2019). Chemistry and Biological  
577 Activities of Processed *Camellia sinensis* Teas: A Comprehensive Review. *Comprehensive*  
578 *Reviews in Food Science and Food Safety*, 18(5), 1474–1495. [https://doi.org/10.1111/1541-](https://doi.org/10.1111/1541-4337.12479)  
579 [4337.12479](https://doi.org/10.1111/1541-4337.12479)

580 Zhang, L., Zeng, Z., Zhao, C., Kong, H., Lu, X., & Xu, G. (2013). A comparative study of volatile  
581 components in green, oolong and black teas by using comprehensive two-dimensional gas  
582 chromatography–time-of-flight mass spectrometry and multivariate data analysis. *Journal of*  
583 *Chromatography A*, 1313, 245–252. <https://doi.org/10.1016/j.chroma.2013.06.022>

584 Zhao, H., Zhang, S., & Zhang, Z. (2017). Relationship between multi-element composition in tea  
585 leaves and in provenance soils for geographical traceability. *Food Control*, 76, 82–87.  
586 <https://doi.org/10.1016/j.foodcont.2017.01.006>

587 Zhou, Z., Wu, Q., Yao, Z., Deng, H., Liu, B., Yue, C., Deng, T., Lai, Z., & Sun, Y. (2020). Dynamics of ADH  
588 and related genes responsible for the transformation of C<sub>6</sub>-aldehydes to C<sub>6</sub>-alcohols during  
589 the postharvest process of oolong tea. *Food Science & Nutrition*, 8(1), 104–113.  
590 <https://doi.org/10.1002/fsn3.1272>